

Design and Validation of an Asymmetric Bowden-Cable-Driven Series Elastic Actuator

Ning Sun, Long Cheng, Lin Tian, Zeng-Guang Hou and Min Tan

Abstract—Weight, size and torque control for hand exoskeleton robots are challenging due to lack of small and compact bidirectional torque actuators. In this paper, an asymmetric Bowden-cable-driven series elastic actuator (ABLE-SEA) for hand exoskeleton robots was proposed based on the fact that the required torques for finger movements are asymmetric. Compared to series elastic actuator and transmission system that were designed separately, the elastic elements of ABLE-SEA were placed in transmission parts to connect series elastic actuator with transmission system, which makes system compact. ABLE-SEA is $71\text{mm} \times 19.5\text{mm} \times 20\text{mm}$ in dimension and weighs 30g except motor which is placed remotely. The dynamic model of ABLE-SEA was established, and feedback proportional-derivative (PD) control plus a feed-forward term was used to track the reference torque for the ABLE-SEA. The reference torque tracking test at different frequencies was performed at the developed prototype. Meanwhile, the peak torque of ABLE-SEA was tested. The experimental results verified that the torque bandwidth of the proposed series elastic actuator could reach 4Hz, and the peak torque of ABLE-SEA could reach 0.3Nm, which meet the design requirement.

I. INTRODUCTION

In recent years, stroke affects a substantial portion of human beings, which leads to limb movement disorder such as hand [1]. Hand exoskeleton robots are a widely growing research hotspot for hand performance rehabilitation, for example, a pneumatically-actuated hand rehabilitation device was proposed to assist in finger extension [2]. When designing hand exoskeleton robots that interact with a human being, safety concerns are essentially considered from control means and physical human-robot coupling system [3]. Some control means have been designed to avoid harm to human. A stability-guaranteed variable impedance control approach for robots was proposed to achieve precise control of force [4]. An admittance control based on the measure force was presented to deal with a human subject's intention [5]. Two composite learning impedance controllers were proposed to improve safety and compliance [6]. A learning impedance controller was designed to obtain desired robot-environment interaction force [7]. And a novel BLF-based adaptive impedance control was proposed to make the robot behavior flexible and adaptive [8]. For motors, there are two main methods for the precise control of torque: torque sensor and feedback control, series elastic actuator (SEA)

This work was supported in part by the National Natural Science Foundation of China (Grants 61873268 and 61633016) and Beijing Natural Science Foundation (Grant L182060).

The authors are with the State Key Laboratory of Management and Control for Complex Systems, Institute of Automation, Chinese Academy of Sciences, Beijing 100190, China. Email: long.cheng@ia.ac.cn. The authors are also with the University of Chinese Academy of Sciences.

and position control with feedback. Compared to the SEAs, adding torque sensor is costly and requires more space, which makes this scheme infeasible for hand exoskeleton robots. And the elastic elements of SEAs make system stiffness decreased, which is beneficial to protect human [9]. However, lightness, miniature and bidirectional SEAs for hand exoskeleton robots are challenging.

SEAs for precisely controlling torque have been successfully applied to the hand exoskeleton robots [10,11]. There are two different categories about SEAs based on location of the motor: (i) locally placed motor, (ii) remotely placed motor.

Baldoni *et al.* presented two different types of miniaturized SEAs with a locally placed motor in order to meet the weight, stiffness and torque requirements of hand exoskeleton robots [10]. Ates *et al.* developed a cheap, miniaturized SEA with a helical torsion spring and a locally placed RC servo, which explored performance characteristics of the hand ServoSEA [12]. Jo and Bae proposed an SEA with a small locally placed linear motor and linear compressed spring to achieve force-control, which has been applied to hand exoskeleton system [13]. Bianchi *et al.* designed a novel SEA with a locally placed motor and structure spring that was designed through the innovative topology optimization method, to achieve a suitable compliance [14]. However, locally placed motor in all these schemes makes the SEA cumbersome.

To overcome this limitation, Agarwal and Deshpande developed two types of SEAs to achieve bidirectional force control, which was actuated by a remotely placed motor and a Bowden-cable-driven transmission [11]. While the SEAs with a remotely placed motor make system lightness, pre-tightening mechanism for eliminating the gap of cable driven is encumbrance. For solving this problem, Jung and Bae proposed an asymmetric cable-driven SEA for the upper exoskeleton robot based on the fact that required joint torques for elbow motion are asymmetric [15]. The gap of cable driven could be eliminated by control method. However, it is questionable because the spring manufacturer said that one helical torsion spring in this SEA can hardly generate bidirectional torque. Meanwhile, the SEA for elbow joint could not be directly applied to hand exoskeleton robots. Note that SEAs and transmission system were designed separately in previous hand exoskeleton robots, which is not good of making system compact.

In this paper, an asymmetric Bowden-cable-driven series elastic actuator (ABLE-SEA) for hand exoskeleton robots was designed based on two linear compressed springs to achieve bidirectional force control. An asymmetric Bowden-

cable-driven mechanism was applied based on the fact that the required torques for finger movements are asymmetric [16]. Meanwhile, compared to previous SEAs, the elastic elements of proposed SEA were placed in transmission parts to meet the requirement of integrating the SEA with the transmission system, which can make the hand exoskeleton robot light and compact.

This paper is organized as follows. In Section II, the design requirement of ABLE-SEA, the Bowden-cable-driven mechanism and the developed prototype are described. In Section III, the dynamic model and control structure of ABLE-SEA are presented. Experimental results of tracking desired torques at several frequencies are shown in Section IV. In Section V, conclusions and future work are provided.

II. MECHANICAL DESIGN

A. Requirements of Design

To assist patients with hand dysfunction to carry out finger rehabilitation training, ABLE-SEA as the actuation element of the hand exoskeleton robot needs to satisfy application requirements such as providing adequate active torque, tracking desired torques at required frequency, the dimension and weight. The design requirements for ABLE-SEA need to be specifically met as follows:

- Peak torque ($\geq 0.3\text{Nm}$): according to the fact that at least 0.3N/m in bidirectional torque is provided by experienced therapists [17], the peak torque requirement is determined.
- Frequency ($\geq 2\text{Hz}$): the rehabilitation exercises of human fingers are performed at frequencies below 0.5Hz [18]. However, the frequency of force compliance control loop in human fingers is $1\text{-}2\text{Hz}$. Therefore, the torque frequency is chosen to be at least 2Hz [19,20].
- Dimension (width $\leq 20\text{mm}$): the dimension of the SEA is required by the fact that two SEAs should be placed in the space whose width is like a finger in order to be applied for multiple fingers adjacent to each other [21].
- Weight ($\leq 30\text{g}$): the weight of each SEA is less than 30g excepting motor, Bowden cable sheaths and Bowden cables [21].

B. Bowden-Cable-Driven Mechanism

The torque generated by the motor is transmitted through the Bowden-cable-driven transmission. The actuation of one DOF rotational joint is required in bidirectional motion, however, the force can only be transmitted by pulling the cable. To meet such requirements, three structures in Fig. 1 have been developed as Bowden-cable-driven mechanism.

The first Bowden-cable-driven mechanism shown in Fig. 1(a) is that each cable is independently pulled by one motor. This mechanism has advantages such as high performance and ease to eliminate the gap by providing the appropriate cable tension. However, the number of motor is more than other mechanisms, which is costly and requires more space.

For solving this issue, the second mechanism (Fig. 1(b)) that one joint is actuated by one motor has been developed. And it has been applied for exoskeleton systems because of

its simple structure [22,23]. For example, a wearable hand rehabilitation with the second mechanism was proposed to achieve the flexion and extension of fingers [24]. Transmission clearance often exists in the cable of the non-pulled side on account of eliminating the tension of the cable, which causes slow response and backlash. Therefore, it is essential to add pretensioning mechanisms in the hardware. Mechanical components (for example, spring, tensioner pulley and screws) were applied to provide the appropriate cable tension. Therefore, such mechanical components cause the Bowden-cable-driven mechanism cumbersome and heavy, and the frequent adjustment required for maintaining appropriate cable tension.

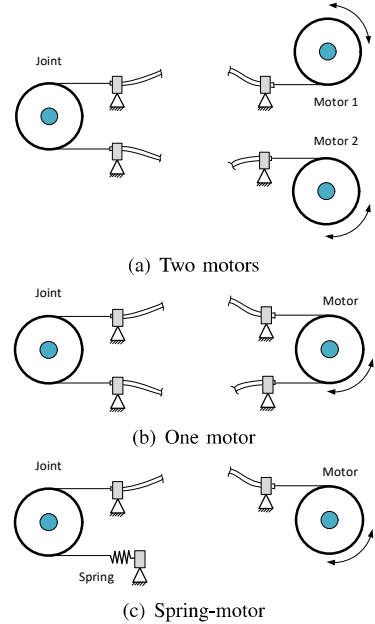


Fig. 1: The three structures of Bowden-cable-driven mechanism. (a) Two motors. (b) One motor. (c) Spring-motor.

Finally, the spring-actuator mechanism presented in Fig. 1(c) was developed based on the method that pre-loading elements of Bowden-cable-driven mechanism were integrated with actuators. Such mechanism uses a motor for the actuation of one side, while the other side is driven by an antagonistic spring. The spring is pre-loaded by compressing it in the installation to use bidirectional forces to the joint. It is the fact that the output force of joint is asymmetric in the spring and motor side. The pre-loaded force and stiffness of springs determine the value of force in the spring side, while the output force of joint in the motor side is determined by subtracting the compressed spring force from the output force of motor. Because the motor needs to compress the spring, the driving force of motor for joint output is smaller than other mechanisms when the same motor is chosen. Nonetheless, transmission clearance can be eliminated, because the cable tension can be maintained appropriately by the pre-load of spring and the motor without additional mechanical components. The more important thing is that

the required joint torques of finger motions are asymmetric. The conclusion is that the spring-actuator mechanism shown in Fig. 1(c) is suitable for the transmission mechanism of hand exoskeleton robotics.

C. Design of ABLE-SEA

The force between human and machine is generated by the deflection of elastic elements. To estimate the force, angle sensors need to be chosen to measure the deflection of elastic element, which should be small enough in dimension due to a small placed space. It is essential that the angular deflection of elastic elements needs to be sufficiently large because of the poor resolution of small angle sensors. Low stiffness of elastic elements should be designed, while higher torque bandwidths and peak torques require high stiffness. Therefore, the choosing of appropriate elastic elements of SEA is distinctly a challenge.

There are three different types of springs: (i) structural torsion spring, (ii) helical torsion spring, (iii) linear compressed spring. Structural torsion spring is usually high stiffness with small angular deflection. For helical torsion springs with linear bidirectional feature of the torque, it is a challenge for SEAs to achieve high stiffness and reasonable placed dimension in outer diameter and width. For example, an SEA with helical torsion spring was developed for hand exoskeleton robot, however, it could not be placed in the space whose width is like a finger [11]. For linear compressed springs, the dimension in length is larger and buckling of the spring often exists. However, these problems could be solved by proper design. From the above discussion, the linear compressed spring is finally chosen for the ABLE-SEA.

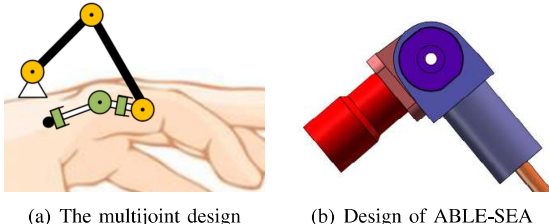


Fig. 2: Design of ABLE-SEA based on the multijoint design.
(a) The multijoint design. (b) Design of ABLE-SEA.

The rotation axes of finger joints are uncertain because of the existence of the soft tissue. A misalignment between the human and robot rotation axes could exist, causing undesired force between human and robot. As shown in Fig. 2(a), the multijoint design is widely applied to avoid misalignment between the human and robot rotation axis [22]. It is obvious that the length of the link in the multijoint design is long. According to this feature, two linear compressed springs are located in the link. This arrangement integrates series elastic actuator with transmission system, which makes the system compact and avoids buckling of the spring. ABLE-SEA shown in Fig. 2(b) is designed. ABLE-SEA is $71\text{mm} \times 19.5\text{mm} \times 20\text{mm}$ in dimension and weighs 30g except motor

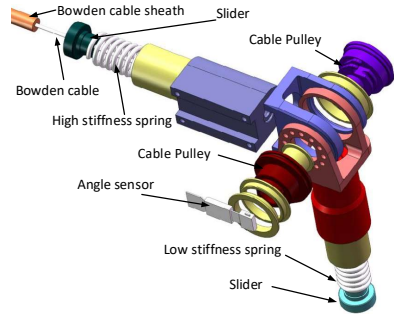


Fig. 3: The elements of ABLE-SEA.

which is placed remotely. The spring-motor mechanism is applied.

The elements of ABLE-SEA are demonstrated in Fig. 3. Bowden cable and Bowden cable sheath are applied to transmit the force generated by the motor. Two linear compressed springs are placed in the link to make system compact, which is connected to the link and the slider. The slider slides in the axial direction of the link, which avoids buckling of the spring. Linear compressed springs are installed and arranged in a different pre-stressed state to generate opposing torques. This configuration ensures that the actuation of one side is driven by a motor and spring, while the other side is driven by an antagonistic spring. A small angle sensor is placed in the joint axis. The deflection of spring could be maintained by using the motor and joint position measurements of the ABLE-SEA.

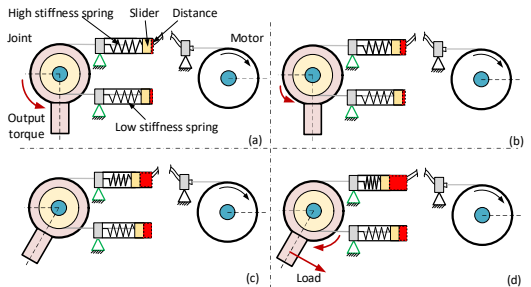


Fig. 4: The motion principle of ABLE-SEA. (a) Initial state and the peak output torque in counterclockwise direction. (b) The output torque in counterclockwise direction. (c) Change the position of the load link. (d) The output torque in clockwise direction.

As shown in Fig. 4, the principle of ABLE-SEA is described. The deflection of linear compressed springs is expressed in dotted box with red area. The magnitude and direction of torque are shown in the length and direction of arrow, respectively. There are two outputs in ABLE-SEA: the position of output link and the torque of output link generated to other objects. There are four cases as follows:

- The initial state is shown in Fig. 4(a). The peak output torque of ABLE-SEA in counterclockwise direction is maintained, which is provided by the pre-load of low stiffness linear compressed spring.

- To maintain the desired output torque of ABLE-SEA counterclockwise, the high stiffness linear compressed spring is compressed by the motor until the output torque of the joint reaches the desired torque (Fig. 4(b)).
- Figure 4(c) shows that when the joint torque in the side of motor is equal to that in the side of spring, the position of the load link would change. The output static torque of ABLE-SEA is zero.
- As shown in Fig. 4(d), when the load is applied and the output torque of joint in clockwise direction is required, the high stiffness linear compressed spring in the side of motor is continuously compressed until meeting the desired torque. Note that the position of output link is constant in this process.

III. SYSTEM MODEL AND CONTROLLER DESIGN

A. System Model

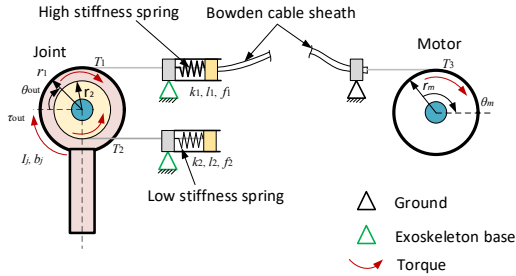


Fig. 5: Schematic of ABLE-SEA.

The schematic of proposed SEA is presented in Fig. 5. In the developed system, the position of actuator should be controlled precisely as the desired torque could be transmitted to the human. The dynamics of the joint end of ABLE-SEA is given by the following equation:

$$I_j \ddot{\theta}_{\text{out}} + b_j \dot{\theta}_{\text{out}} - \tau_{\text{out}} = T_1 - T_2, \quad (1)$$

where I_j is the inertia of output link of ABLE-SEA, b_j is the damping coefficient at the proposed SEA joint, τ_{out} is the output torque of ABLE-SEA, θ_{out} is the joint angle of output link of the developed SEA, T_1 and T_2 are the torque generated by the tension of each Bowden cable to rotation axis of joint. Particularly, the torques generated by the cables tension are calculated as follows:

$$\begin{aligned} T_1 &= (k_1 \Delta l_1 + f_1) r_1, \\ T_2 &= (k_2 \Delta l_2 + f_2) r_2, \end{aligned} \quad (2)$$

where k_1 and k_2 are the stiffness of two linear compressed springs, respectively, Δl_1 and Δl_2 represent the change in length of two linear compressed spring, f_1 and f_2 are the pre-load of two linear compressed spring, r_1 and r_2 denote the radius of ABLE-SEA joint pulley. Friction generated by Bowden-cable-driven mechanism could not be considered in the dynamics equation, because the sheath with low friction inner tube was chosen. The motor as a position source (the output position of the motor is precise) is modeled here, because the effects of force noise are minimized when

controlling the position of motor. In addition, the position control loop at the motor level runs at several thousand Hertz, while the torque control loop runs at 500Hz. The bandwidth for the finger rehabilitation exercises (full flexion and extension) is below 0.5Hz. According to all these factors, the motor dynamics is not considered.

The kinematic relationship about the high and low stiffness compressed springs (suppose the deflection of Bowden cable and Bowden cable sheath at the load is ignored) is given as follows:

$$\begin{aligned} \Delta l_1 &= \theta_m r_m - \theta_{\text{out}} r_1, \\ \Delta l_2 &= \theta_{\text{out}} r_2, \end{aligned} \quad (3)$$

where θ_m is the output angle of motor, r_m is motor pulley radius. The output torque between human and machine generated by the deflection of the spring is described by the following equation:

$$-\tau_{\text{out}} = [k_1(\theta_m r_m - \theta_{\text{out}} r_1) + f_1]r_1 - (k_2 \theta_{\text{out}} r_2 + f_2)r_2. \quad (4)$$

Therefore, the feed-forward motor position (θ_{mf}) with a given desired torque (τ_{aim}) is calculated as follows:

$$\theta_{mf} = \frac{(k_2 \theta_{\text{out}} r_2 + f_2)r_2 - (f_1 - k_1 \theta_{\text{out}} r_1)r_1 - \tau_{\text{aim}}}{k_1 r_m r_1}. \quad (5)$$

In practice, the stiffness and pre-load of springs are not equal to the theoretical ones, and friction, stick-slip, and reflected inertia through a transmission make the model inaccurate. Hence, proper controllers should be designed to overcome these problems.

B. Controller Design

For solving the tracking problem of ABLE-SEA, the feedback proportional-derivative (PD) control plus a feed-forward term has been designed to track the reference torque of the ABLE-SEA driven joint. As shown in Fig. 6, the developed controller includes an inner position control loop at the motor level and an outer torque control loop at the ABLE-SEA level. The feedback PD controller is given by the following equation:

$$u = k_p e + k_d \dot{e} + \theta_{mf}, \quad (6)$$

where u is the control input for the motor system, k_p and k_d are the proportional and derivative gains of the feedback PD controller, respectively, $e = \tau_{\text{aim}} - \hat{\tau}_{\text{out}}$ is the error between ABLE-SEA joint output torque and the desired torque, and $\hat{\tau}_{\text{out}}$ is the estimated torque. The feed-forward term θ_{mf} denotes the model-based input for the desired output. The feed-forward term is beneficial to enhance the control stability and accuracy [25].

According to Fig. 6, the closed-loop transfer function for the control system takes the form as the following equation:

$$\begin{aligned} G_c(s) &= \frac{\tau_{\text{out}}}{\tau_{\text{aim}}} \\ &= \frac{G_{mc}(s)G_m(s)G_{SEA}(s)(G_f(s) + G_{PD}(s))}{1 + G_{mc}(s)G_m(s)(1 + G_{SEA}(s)G_{PD}(s))}, \end{aligned} \quad (7)$$

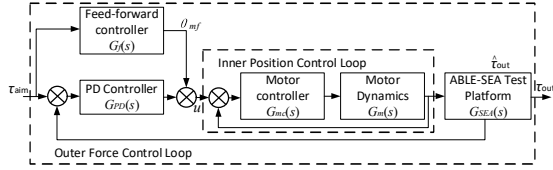


Fig. 6: The schematic of feed-forward PD applied to the ABLE-SEA test platform.

where $G_c(s)$ is the closed loop transfer function of the developed system, $G_{mc}(s)$ represents the motor controller's transfer function, $G_m(s)$ is motor's transfer function, $G_{SEA}(s)$ is ABLE-SEA's transfer function, $G_{PD}(s)$ denotes the feedback component of the controller's transfer function, $G_f(s)$ is the feed-forward component of the controller's transfer function.

IV. EXPERIMENT

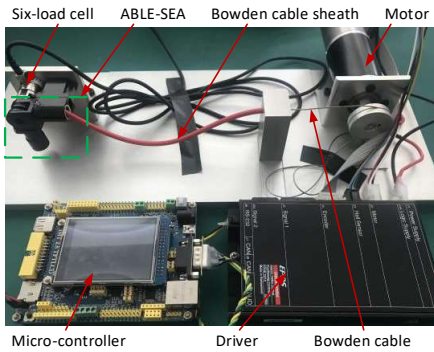
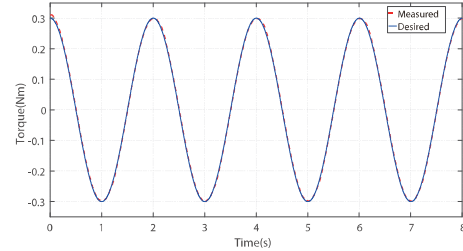


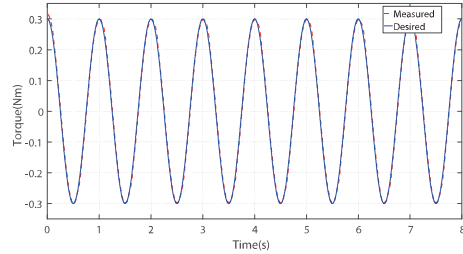
Fig. 7: The rest platform based on proposed SEA.

As shown in Fig. 7, a test platform based on the developed SEA is built. Micro-controller is applied to transfer the control instruction to the motor driver (ESCON 70/10, Maxon). A Maxon motor (EC-i 40, Maxson) with planetary gearbox (reduction ratio 74:1) and encoder (Encoder 16 EASY) is chosen. Metal sheath with PTEE inner tube is used to reduce the losses in the transmission, and the diameter of Bowden steel cable is 0.8mm. Linear compressed springs are chosen from Leespring. The stiffnesses of linear compressed springs are 8.91Nmm and 5.83Nmm respectively. A small magnetic angle sensor (KMA210, NXP Semiconductors) is installed on the ABLE-SEA to measure the output angle of joint. The noise of magnetic angle sensor is approximately 0.5 deg at the peak magnitude, which is acceptable for estimating output torque [11]. The output link of ABLE-SEA is connected to a six-load cell (Nano 17, ATI) to measure the output torque of joint. The six-load cell is connected to PC by data acquisition card to transfer data to PC. And the output torque of joint would be transferred to the micro-controller through the serial port.

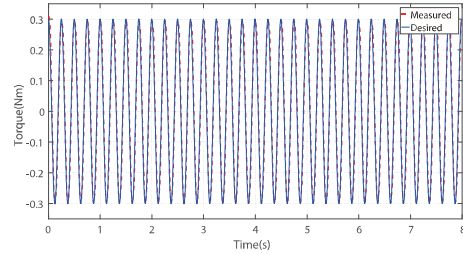
Based on the test platform, several sinusoidal desired joint torques with the same peak torque and different frequencies are tracked in order to test peak torque and torque bandwidth



(a) Tracking sinusoidal desired torque with 0.5Hz



(b) Tracking sinusoidal desired torque with 1Hz



(c) Tracking sinusoidal desired torque with 4Hz

Fig. 8: Tracking sinusoidal desired torque with different frequencies and the peak torque is 0.3Nm. (a) Tracking sinusoidal desired torque with 0.5Hz. (b) Tracking sinusoidal desired torque with 1Hz. (c) Tracking sinusoidal desired torque with 4Hz

of the proposed SEA. The frequencies of sinusoidal desired joint torque are 0.5Hz, 1Hz, and 4Hz respectively, and the peak torque of sinusoidal desired joint torque is 0.3Nm. Note that the output link is connected to the six six-load cell, and the output angle of joint is constant due to the small deformation of six-load cell. When the test runs, the output angle of joint is 30°. Note that the position of the output link does not affect the torque bandwidth of ABLE-SEA, because it is determined by the stiffness of spring.

The results are demonstrated in Fig. 8, and the results of tracking the desired sinusoidal joint torque with 0.5Hz, 1Hz and 4Hz are exhibited by Fig. 8(a), Fig. 8(b), Fig. 8(c), respectively. The red dotted line stands for the desired torque, and the blue line stands for the measured torque. The results verified that the torque bandwidth of ABLE-SEA could reach 4Hz and the peak torque of ABLE-SEA is 0.3Nm. The torque bandwidth of existing SEA proposed for hand exoskeleton robot in [10] and [21] is also 4Hz, and the peak torque of the proposed SEA in [10] and [21] is 0.2Nm and 0.3Nm, respectively. The bending force of Bowden-cable

sheath shows some deviations of the measured trajectory due to choosing short Bowden-cable sheath. Also, the stiffness and pre-load of linear compressed spring in practice are not equivalent to the theoretical values.

V. CONCLUSIONS

In this paper, an asymmetric Bowden-cable-driven series elastic actuator for achieving the force control of hand exoskeletons is proposed. According to the fact that the required torques of finger movements are asymmetric, the spring-motor mechanism is applied to the developed SEA, which uses a motor for the actuation of one side, while the other side is driven by an antagonistic spring. And the linear compressed springs of the proposed SEA are placed in the transmission parts, which integrates series elastic actuator with transmission system. This feature can make the system compact. The dynamics of ABLE-SEA is established, and the feedback proportional-derivative control plus a feed-forward term is designed to track the desired torque. A test platform is designed to test the torque bandwidth and peak torque of the developed SEA. The experimental results show that the torque bandwidth of ABLE-SEA could reach 4Hz and the peak torque of ABLE-SEA could reach 0.3Nm. The proposed prototype is able to be applied to hand exoskeleton robotics.

In the future, some key parameters of the ABLE-SEA such as the stiffness and pre-load of springs in practice should be identified to estimate the output torque of joint. The exoskeleton system for a finger is to be designed based on the developed SEA. The finger rehabilitation training was carried out according to the hand gestures recognized by spiking neural network [26] or BP neural network [27]. And a stretchable strain sensor will be studied to detect the position of the joint [28].

REFERENCES

- [1] E.J. Benjamin, S.S. Callaway, *et al.*, "Heart disease and stroke statistics-2018 update: a report from the American Heart Association," *Circulation*, vol. 137, no. 12, pp. 67-492, Mar. 2018.
- [2] H.C. Li, L. Cheng, "Preliminary study on the design and control of a pneumatically-actuated hand rehabilitation device," in *Proceedings of the 32nd Youth Academic Annual Conference of Chinese Association of Automation*, Hefei, China, May, 2017, pp. 860-865.
- [3] H. Vallery, J. Veneman, E.V. Asseldonk, R. Ekkelenkamp, M. Buss, and H.V.D. Kooij, "Compliant actuation of rehabilitation robots," *IEEE Robotics and Automation Magazine*, vol. 15, no. 3, pp. 60-69, Sept. 2008.
- [4] T.R. Sun, L. Peng, L. Cheng, Z.G. Hou, and Y.P. Pan, "Stability-guaranteed variable impedance control of robots based on approximate dynamic inversion," *IEEE Transactions on Systems, Man, and Cybernetics: Systems*, DOI: 10.1109/TSMC.2019.2930582, Aug. 2019.
- [5] Z.J. Li, B. Huang, Z.F. Ye, M.D. Deng, and C.G. Yang, "Physical human-robot interaction of a robotic exoskeleton by admittance control," *IEEE Transactions on Industrial Electronics*, vol. 65, no. 12, pp. 9614-9624, Mar. 2018.
- [6] T.R. Sun, L. Peng, L. Cheng, H.G. Hou, and Y.P. Pan, "Composite learning enhanced robot impedance control," *IEEE Transactions on Neural Networks and Learning Systems*, DOI: 10.1109/TNNLS.2019.2912212, May. 2019.
- [7] T.R. Sun, L. Cheng, L. Peng, Z.G. Hou, and Y.P. Pan, "Learning impedance control of robots with enhanced transient and steady-state control performances," *Science China Information Science*, in press, 2019.
- [8] Z.J. Li, B. Huang, A. Ajoudani, C.G. Yang, C.Y. Su, and A. Bicchi, "Asymmetric bimanual control of dual-arm exoskeletons for human-cooperative manipulations," *IEEE Transactions on Robotics*, vol. 34, no. 1, pp. 264-271, Nov. 2018.
- [9] A.D. Santis, B. Siciliano, A.D. Luca, and A. Bicchi, "An atlas of physical human-robot interaction," *Mechanism and Machine Theory*, vol. 43, no. 3, pp. 253-270, Mar. 2008.
- [10] A. Baldoni, M. Cempini, M. Cortese, S. Crea, M.C. Carrozza, and V. Nicola, "Design and validation of a miniaturized SEA transmission system," *Mechatronics*, vol. 49, pp. 149-156, Feb. 2018.
- [11] P. Agarwal and A.D. Deshpande, "Series elastic actuators for small-scale robotic applications," *Journal of Mechanisms and Robotics*, vol. 9, no. 3, Jun. 2017.
- [12] S. Ates, V.I. Sluiter, P. Lammertse, and A.H.A. Stienen, "ServoSEA concept: Cheap, miniature series-elastic actuators for orthotic, prosthetic and robotic hands," in *Proceedings of 5th IEEE RAS/EMBS International Conference on Biomedical Robotics and Biomechatronics*, Sao Paulo, Brazil, Aug. 2014, pp. 751-757.
- [13] I. Jo and J. Bae, "Design and control of a wearable and force-controllable hand exoskeleton system," *Mechatronics*, vol. 41, pp. 90-101, Feb. 2017.
- [14] M. Bianchi, M. Conti, R. Meli, A. Ridolfi, N. Vitiello, and B. Allotta, "Design of a Series Elastic Transmission for hand exoskeletons," *Mechatronics*, vol. 51, pp. 8-18, May. 2018.
- [15] Y. Jung and J. Bae, "An asymmetric cable-driven mechanism for force control of exoskeleton systems," *Mechatronics*, vol. 40, pp. 41-50, Dec. 2016.
- [16] S. Brorsson, A. Nilsdotter, E. Pedersen, A. Bremander, and C. Thorstensson, "Relationship between finger flexion and extension force in healthy women and women with rheumatoid arthritis," *Journal of Rehabilitation Medicine*, vol. 44, no. 4, pp. 605-608, Jun. 2012.
- [17] S. Ueki, H. Kawasaki, S. Ito, Y. Nishimoto, M. Abe, T. Aoki, Y. Ishigure, T. Ojika, and T. Mouri, "Development of a hand-assist robot with multi-degrees-of-freedom for rehabilitation therapy," *IEEE-ASME Transactions on Mechatronics*, vol. 17, no. 1, pp. 136-146, Feb. 2012.
- [18] H. Kawasaki, H. Kimura, S. Ito, Y. Nishimoto, H. Hayashi, and Sakaeda, "Hand rehabilitation support system based on self-motion control, with a clinical case report," in *Proceedings of 2006 World Automation Congress*, Budapest, Hungary, Jul. 2006, pp. 1-6.
- [19] T.B. Sheridan and W.R. Ferrell, *Man-Machine Systems: Information, Control, and Decision Models of Human Performance*, MIT Press, 1974.
- [20] R.B. Chan and D.S. Childress, "On information-transmission in human-machine systems-channel capacity and optimal filtering," *IEEE Transactions on Systems Man and Cybernetics*, vol. 20, no. 5, pp. 1136-1145, Sept. - Oct. 1990.
- [21] P. Agarwal, J. Fox, Y. Yun, M.K.O. Malley, and A.D. Deshpande, "An index finger exoskeleton with series elastic actuation for rehabilitation: Design, control and performance characterization," *International Journal of Robotics Research*, vol. 34, no. 14, pp. 1747-1772, Dec. 2015.
- [22] M. Cempini, M. Cortese, and N. Vitiello, "A powered finger/thumb wearable hand exoskeleton with self-aligning joint axes," *IEEE-ASME Transaction on Mechatronics*, vol. 20, no. 2, pp. 705-716, Apr. 2015.
- [23] H. In, B.B. Kang, M. Sin, and K.J. Cho, "Exo-glove: a wearable robot for the hand with a soft tendon routing system view document," *IEEE Robotics and Automation Magazine*, vol. 22, no. 1, pp. 97-105, Mar. 2015.
- [24] L. Cheng, M. Chen, and Z.W. Li, "Design and control of a wearable hand rehabilitation," *IEEE Access*, vol. 6, pp. 74039-74050, Dec. 2018.
- [25] W.S. Levine, *The Control Handbook*, CRC Press, 1996.
- [26] L. Cheng, Y. Liu, Z.G. Hou, M. Tan, D.J. Du, and M.R. Fei, "A rapid spiking neural network approach with an application on hand gesture recognition," *IEEE Transactions on Cognitive and Developmental Systems*, DOI: 10.1109/TCDS.2019.2918228, May. 2019.
- [27] M. Chen, L. Cheng, F.B. Huan, Z.G. Hou, "Towards robot-assisted post-stroke hand rehabilitation: Fugl-Meyer gesture recognition using sEMG," in *Proceedings of the 7th Annual IEEE International Conference on Cyber Technology in Automation, Control, and Intelligent Systems*, Hawaii, USA, July, 2017, pp. 1472-1477.
- [28] Z.W. Li, Q.K. Song, L. Cheng, M. Tan, "Snoring detection based on a stretchable strain sensor," *Scienece China Information Science*, accepted, 2019.